Improving the packing efficiency of building integrated concentrating photovoltaic systems through a novel hexagonal concentrator

Tamuno-Ibuomi, Lewis Osikibo; Ramirez-Iniguez, Roberto; Holmes-Smith, A. Sheila; Bevan, Geraint

Published in:
2022 57th International Universities Power Engineering Conference (UPEC)

DOI:
10.1109/UPEC55022.2022.9917592

Publication date:
2022

Document Version
Author accepted manuscript

Improving the Packing Efficiency of Building Integrated Concentrating Photovoltaic Systems through a Novel Hexagonal Concentrator

Lewis Osikibo Tamuno-Ibuomi
School of Computing, Engineering and Built Environment
Glasgow Caledonian University
Glasgow, United Kingdom
Ltamun10@gcu.ac.uk

Roberto Ramirez-Iniguez
School of Computing, Engineering and Built Environment
Glasgow Caledonian University
Glasgow, United Kingdom
Roberto.RamirezIniguez@gcu.ac.uk

A Sheila Holmes-Smith
School of Computing, Engineering and Built Environment
Glasgow Caledonian University
Glasgow, United Kingdom
A.S.Smith@gcu.ac.uk

Geraint Bevan
School of Computing, Engineering and Built Environment
Glasgow Caledonian University
Glasgow, United Kingdom
Geraint.Bevan@gcu.ac.uk

***Abstract*— Building Integrated Concentrating Photovoltaic systems have the potential of helping to reduce greenhouse gas emissions and global warming as they can be designed not only to generate electricity but also to improve energy efficiency in buildings. These systems can incorporate static low concentration optics and PV cells within double glazed windows, skylights, and double skin facades. This paper addresses the issue of low packing density of solar concentrators used in low concentrating photovoltaic systems and proposes a novel 3-D hexagonal concentrator which offers 89.4% theoretical packing efficiency, which is 16.2% and 21.8% higher than the theoretical packing efficiencies of the circular and elliptical concentrators respectfully, the alternative 3-D concentrators discussed in this study.**

Keywords*— *low concentrating photovoltaic, packing density, efficiency, 3-D, hexagonal concentrator.

I. INTRODUCTION

Energy is essential and serves as the mainstay of a nation's economic development and growth, most of which is utilised within the built environment. Buildings, which are the largest consumers of electricity, have high energy saving potential and can therefore contribute to reducing greenhouse gas (GHG) emissions [1]. This can be achieved if buildings are equipped with the necessary renewable energy source technology such as solar photovoltaic (PV), which is the most popular renewable energy technology that has been applied to buildings since the 1970s [2].

Building integrated concentrating photovoltaic (BICPV) systems are particularly attractive as they can be integrated into the building envelope. This means that elements of the BICPV system can be used to replace structural elements of a building, and thus, offset some of the cost whilst helping to improve its aesthetics [3].

The main element of the BICPV technology is the concentrating photovoltaic (CPV) unit, which consists of a low-cost optical material that can concentrate sunlight by directing it from a wider entrance aperture to a smaller exit aperture where a solar cell is attached. The ratio of the entrance aperture area to the exit aperture area of a three-dimensional (3-D) concentrator is termed the geometrical concentration ratio (CR). It is used in defining the concentrator type, and based on that, three classifications exist: (i) low concentration devices (CR < 10) (ii) medium concentration devices (10 ≤ CR < 100) and (iii) high concentration devices (CR ≥ 100). For most BICPV applications, low concentrating photovoltaic devices are used and are therefore, referred to as building integrated low concentrating photovoltaic (BILCPV) systems. These are normally static (no electromechanical tracking required) and use 3-D, nonimaging optics, which are found more suitable than their 2-D counterparts [4].

Several aspects of the BICPV technology have been investigated over the years, but the one that has received little attention is the packing density of the concentrators within static low concentrating photovoltaic (LCPV) systems. This issue can have an effect on the overall performance. A low packing density, for instance, limits the number of concentrators (and PV cells) on a given area. Large spaces between the concentrators in a CPV module are an indication of low packing density, and a potential loss of convertible solar energy. In [5], the authors attempted to rearrange the concentrators to enhance the packing density, but ended up with an overlap of the concentrators' entrance aperture areas, which introduces shading and alignment issues as shown in Fig. 1.

In another example stated in [2], the authors presented the fabrication of a novel 3-D optical concentrator for building integration and named it translucent solar concentrator but the solar window prototypes indicate low packing density which was not addressed in their work. This is illustrated in Fig. 2.

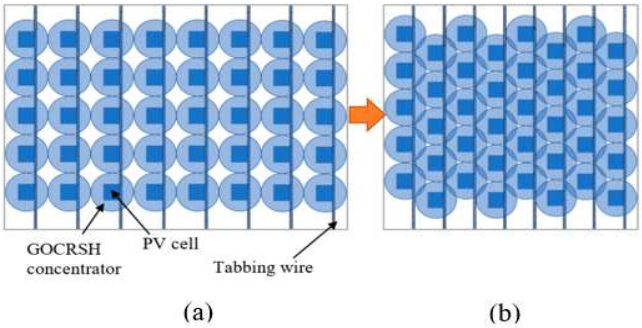

Fig. 1. Genetically optimized circular rotational square hyperboloid concentrator (GOCRSH) module top view (a) with low packing density (b) with enhanced packing density, but overlapped concentrators [5].

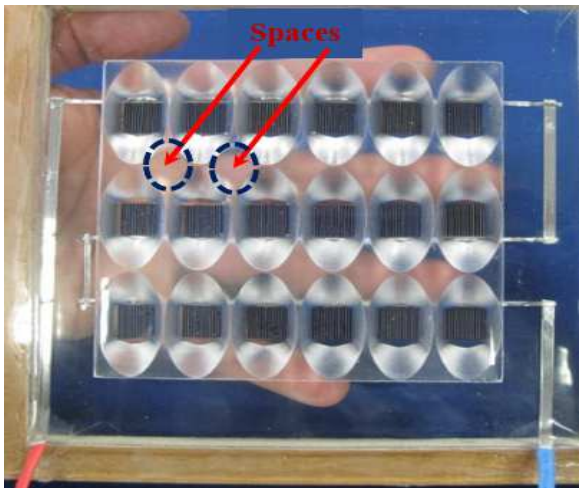

Fig. 2. Solar window of a translucent solar concentrator called square elliptically hyperboloid (SEH) concentrator by the authors [2].

There are, however, a few designs which indicate a high packing density factor. For instance, in [6], the 3-D reflective cross compound parabolic concentrator (3-D CCPC) for BICPV application has a square entrance aperture which promises a very high packing density. A similar performance would be expected with a concentrator having a rectangular entrance aperture.

This paper, thus, presents the design and development of a novel LCPV device for BICPV application, which provides improved packing density with the aim of enhancing the performance of the concentrator.

II. Conceptal Design Considerations

A. *Conventional entrance aperture geometries of 3-D BILCPV concentrators*

Some of the common conventional entry area geometries, adopted in designing LCPV systems are shown in Fig. 3-5. Each module consists of nine concentrators.

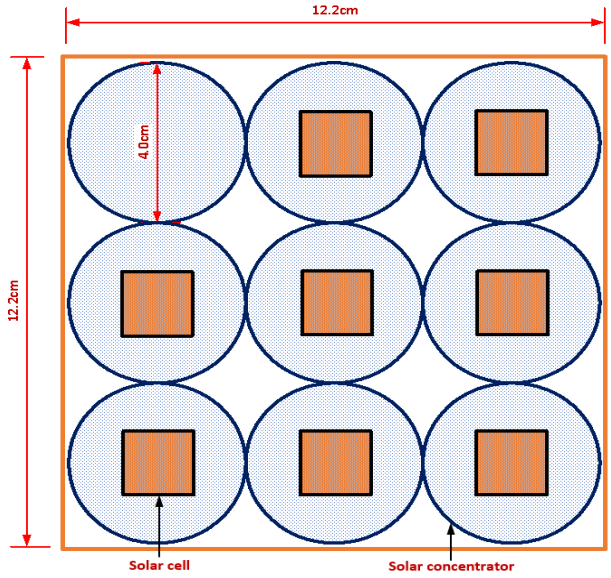

Fig. 3. Circular entrance aperture geometry adopted in LCPV designs

Examples of 3-D optics with a circular entrance geometry shown in Fig. 3 can be found in [3] and [5]. The 3-D compound parabolic concentrator (CPC), widely used, has a circular entrance aperture.

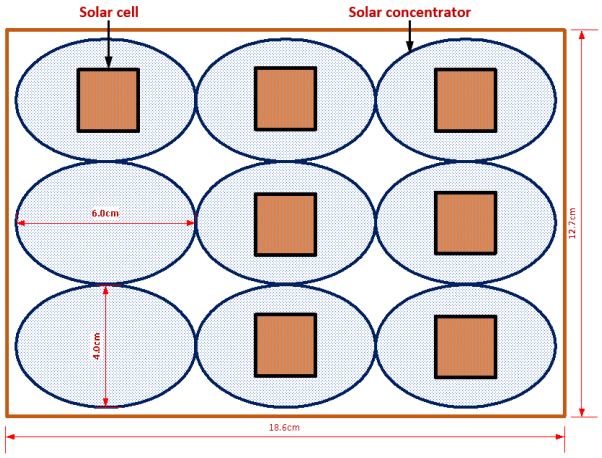

Fig. 4. Elliptical entrance aperture geometry adopted in LCPV designs

An example of 3-D optics with an elliptical entrance geometry, shown in Fig. 4, is the square elliptically hyperboloid (SEH) concentrator, presented in [2].

An example of 3-D optics with a square entrance geometry given in Fig. 5 is already discussed, designed and produced in [6].

B. *Definition of packing density for BILCPV systems*

The entrance aperture in LCPV devices may be flat or dome-shaped as stated in [4]. The aspect of the concentrator concerned with packing density is mainly the entrance geometry, preferably flat for the following reasons: (i) compactness, (ii) ease of assembly, (iii) uniformity of irradiance distribution across the concentrators' solar capture area, (iv) cost-effectiveness, and (v) stable surface albedo.

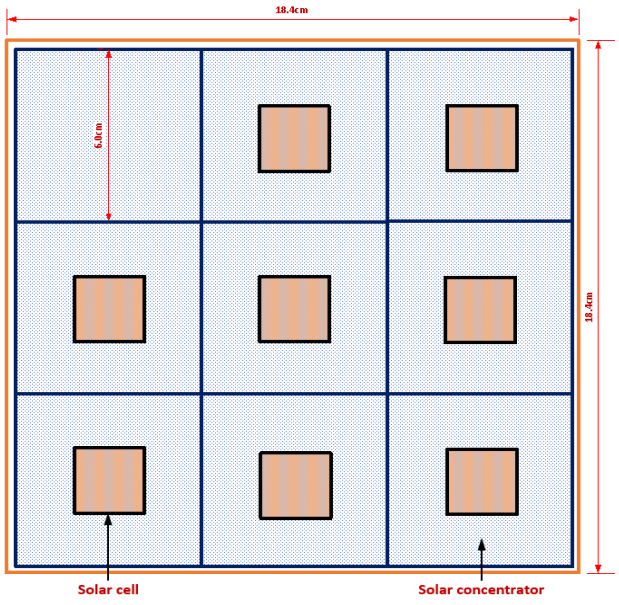

Fig. 5. Square (or rectangular) entrance aperture geometry adopted in LCPV designs

In this work, packing density is defined as the proportion of the total module area occupied by the solar concentrators' capture area. Packing density is therefore, related to the amount of gap-free area among the entrance apertures within

a static LCPV module when viewed from the top as shown in Fig. 3. In order to compare and evaluate the packing densities of various concentrators, the packing efficiency (eff_{Pd}) is used instead, and this can be determined mathematically, at constant height, as follows:

$$eff_{Pd} = (N_{sc} \bullet A_{sc}) / A_{ms} \bullet 100\%. \quad (1)$$

where N_{sc} is number of solar concentrators, A_{sc} is the entrance aperture area of a concentrator in the module and A_{ms} is the total module surface area.

The packing efficiency is used to determine the exact number of concentrators for optimal performance within the module. Another parameter defined in this work is the potential loss of convertible solar energy which is mathematically stated as given in (2).

$$L_{sc} = (A_{ms} - (N_{sc} \bullet A_{sc})) / A_{sc} \quad (2)$$

where L_{sc} is the loss factor in potential convertible solar energy within the module and can be used to check for the degree of the module packing density.

Following the outcome of the equations stated above, the solar energy capturability of each solar concentrator within the module with the highest possible packing density can be determined by:

$$C_{sg} = (L_{sc} \bullet A_{sc}) / (N_{sc} \bullet A_{ms}) \quad (3)$$

where C_{sg} is the sun light capturability factor of a concentrator with respect to the total module surface area with a high packing density.

A geometrical concentration ratio of less than 10 is typical for BILCPV applications and is defined for each concentrator as the ratio of the entrance aperture area to the exit aperture area. Therefore, the geometrical concentration gain for the entire solar module can be calculated using equation (4).

$$M_{CR} = (N_{sc} \bullet A_{sc}) / A_{co} \quad (4)$$

where A_{co} is the total exit area of all the solar concentrators within the module.

C. *Possible improvement of packing density by rearranging the concentrators.*

In [5] and Fig. 1, an attempt of rearranging the GOCRSH concentrator to enhance packing density was presented by the authors. Following the same approach, the commonly adopted circular and elliptical geometries given in Figs. 3 and 4 can be rearranged without overlapping to achieve maximum packing density as demonstrated in Figs. 6 and 7.

The whole idea of repositioning the concentrators is to increase the packing efficiency by removing the gaps between the entrance apertures, thus creating a zero-gap

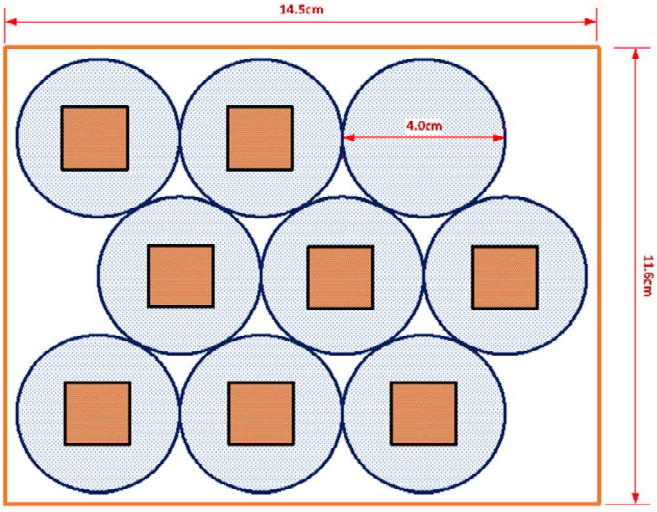

Fig. 6. Repositioning of nine concentrators with circular entrance apertures for possible packing density improvements.

profile. The profiles shown in Figs. 6 and 7, do not produce a zero-gap profile. However, they show the best packing density for the circular and elliptical entrance geometries respectively. When these profiles are compared with the square or rectangular entry geometry of Fig. 5, the concept of packing density becomes very clear. The square entry geometry can be considered as having the best or highest packing density by inspection. This work considers the square entry geometry as an ideal profile and will serve as the basis for comparison with other concentrators within the scope of this work.

The performance of the CPC has been investigated with various polygonal apertures in terms of uniform illumination distribution and in that study, both the entrance and exit had similar geometries. There was however, no mention of packing density all through the study [7]. This work proposes a novel 3-D concentrator with a polygonal entry aperture and a square exit that can improve the packing density of a module close to the zero-gap profile as shown in Figs. 8 and 9.

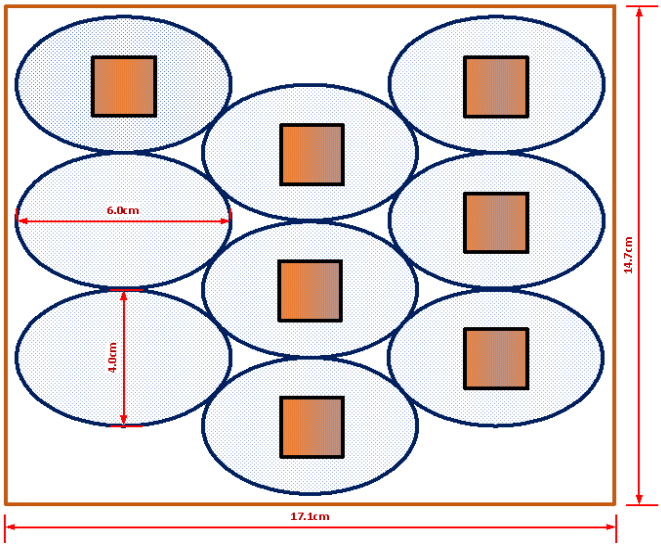

Fig. 7. Rearranging of nine concentrators with elliptical entrance apertures for possible packing density improvements.

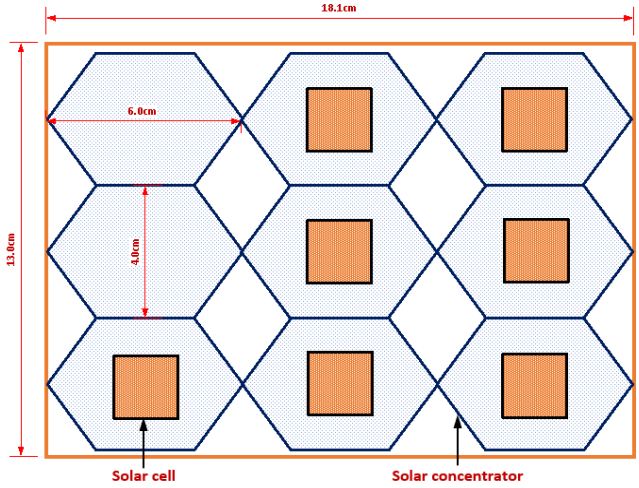

Fig. 8. Novel hexagonal entrance aperture geometry for LCPV applications.

Based on the design considerations outlined earlier, this work adopts a flat hexagonal entrance aperture for the novel 3-D hexagonal (3-D Hex) LCPV design. Fig. 8 shows a module of the 3-D Hex concentrator with nine concentrators, while in Fig. 9, the concentrators are rearranged within the module to achieve the best possible packing density, producing a zero-gap profile.

III. Design and Development of the Novel 3-D Hex Concentrator

Most 3-D nonimaging static concentrators for BILCPV applications are designed based on the edge-ray principle. Recently, modern methods based on parametric equations which enhances numerical optimisation were proposed for modelling 3-D static LCPV devices [8]. In this work, the design method is based on developing parametric equations in 3-D views.

Like any other 3-D concentrators, the Hex concentrator has three views: top view (flat hexagonal entrance), exit aperture view (square), and a side profile view as shown in Fig. 10. The hexagon is assumed to be regular with each of the sides having equal length and angle at the centre equivalent to $\pi/3$. Thus, the regular hexagon consists of six equilateral triangles.

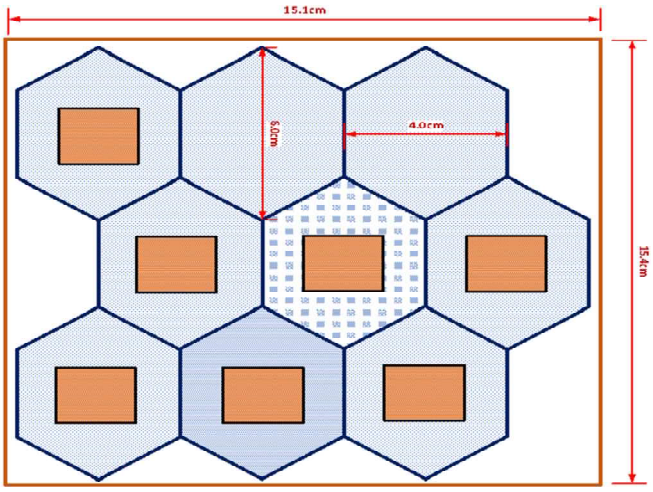

Fig. 9. Rearranging of concentrators with hexagonal entrance apertures for possible packing density improvements

A. Geometrical concentration ratio of the Hex concentrator

The geometrical concentration gain for the 3-D Hex concentrator ($C_{geo\text{-}Hex}$) is determined from Fig. 10 as follows:

$$C_{geo\text{-}Hex} = A_{entrance} / A_{exit} = 3ab / d_0^2 \quad (5)$$

where $a = 2r \sin\theta = d_1 \sin\theta$, $b = r \cos\theta = (d_1/2)\cos\theta$ and $3ab = (3/2)\, d_1^2 \sin\theta \cos\theta$, $A_{entrance}$ is entrance aperture area, A_{exit} is exit aperture area.

$$C_{geo\text{-}Hex} = 3\, ab / d_0^2 = (3/2)\, d_1^2 \sin\theta \cos\theta / d_0^2 \quad (6)$$

But $\theta = 180^0 / n$, where $n = 6$, the number of sides of the regular polygon; $\theta = 30^0$.

$$\therefore C_{geo\text{-}Hex} = (3/8)\,(3)^{1/2}\,(d_1/d_0)^2 \quad (7)$$

[Note: $d_1 = 2r = 2a$]

To achieve a geometrical concentration ratio < 10 × for static LCPV application, keep $a < 1.98$. Thus, by increasing the value of a, the hexagonal concentrator can be used for both medium and high concentration applications.

B. Modelling and design of 3-D Hex concentrator

To define the 3-D hexagonal concentrator cartesian coordinates, the polar coordinates for the x and y axes are first derived for both the hexagonal entrance and square exit geometries. The height profile then completes the third or z axis coordinate. For the polar coordinates, the hexagon and square (both of the polygonal family) are divided into four quadrants as shown in Fig. 11.

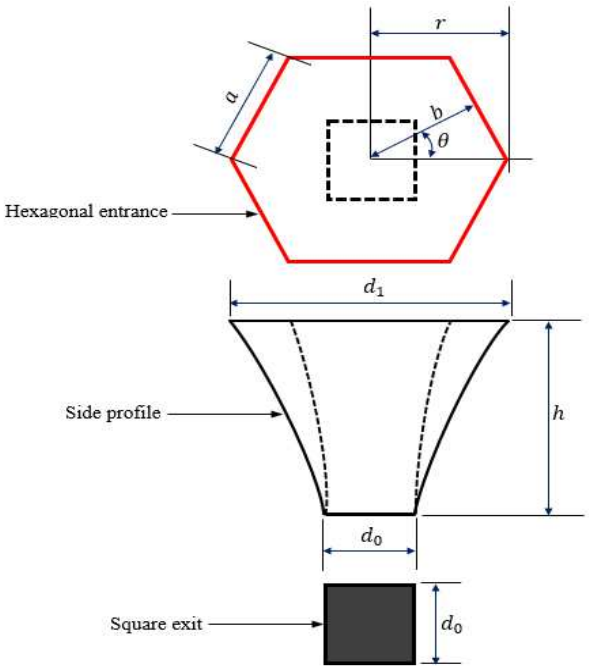

Fig. 10. Orthogonal views of the Hex-concentrator

where a is the length of each side of the regular hexagon, b is the length of the apothem or radius of the inscribed circle, r is the radius of the circumscribed circle, θ is the angle subtended at the centre by b and r, d_1 is the entrance aperture length from the North-South plane, h is the height of the concentrator, and d_0 is the length of each side of the square exit.

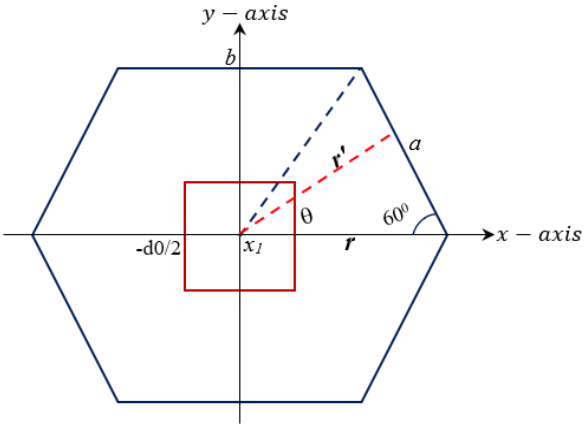

Fig. 11. Quadrant features of a hexagonal entrance and a square exit aperture

A common angle of rotation θ is defined with a changing radius *r'*, which is a function of the rotation angle in the first quadrant. This process is replicated for the remaining quadrants by simply incrementing θ from 0 to 360^0. An array of radii and rotation angles are created using MATLAB and these can be plotted in polar coordinates to observe the share of the coordinate parameters between the hexagonal entrance and square exit. Blending the height profile with these data produces a 3-D hexagonal concentrator with a well-defined hexagonal entrance, square exit, and side profile.

By applying the sine rule to the obtuse triangle formed with the changing radius such that the angle opposite the actual radius *r* is $(120^0 - \theta)$, the equation for the changing radius for both the hexagon and square can be determined as both parameters are proportional and dependent on the rotational angle. Adding a floor function to the equations given in (8) and (9), a 360^0 rotation can be achieved. By multiplying the changing radius with the length of each side of the hexagon (a) or square (d_0), the desired 2-D polar coordinates and plots can be generated.

$$r_{hex}(r', \theta) = \sin 60^0 / \sin(120^0 - \theta) = 0.5a\,(3)^{1/2} / \sin(\theta + 60^0) \quad (8)$$

$$r_{sq}(r', \theta) = 0.5d_0\,(2)^{1/2} / (\cos(\theta + 90^0) + \sin(\theta + 90^0)) \quad (9)$$

where r_{hex} and r_{sq} are the changing radii of the hexagonal entrance and square exit respectively. The polar plot will show the angles at each coordinate and the corresponding radii.

The height is blended with the x and y coordinates according to equation (10).

$$r_c = h \bullet r_{hex} + (1-h) \bullet r_{sq} \quad (10)$$

where r_c forms an array of the combined radius of both the hexagon and square parameters. h is the normalized height, usually given a range from 0 – 1.

The 3-D design builds from bottom to top and the bottom is designed to be a square geometry while the rest of the parts are hexagonal to the desired height, and this creates the side profile. When $h = 0$, the transverse section of the 3-D Hex concentrator is a square, and when $h = 1$, the transverse section is a hexagon. By multiplying the desired height H, by the normalized height h, the total height of the concentrator is determined.

The 3-D coordinates for creating the novel 3-D Hexagonal concentrator in MATLAB are given below.

$$x = r_c \bullet \cos\theta$$
$$y = r_c \bullet \sin\theta$$
$$z = H \bullet h$$

IV. Results and Discussions

A. Packing efficiency calculation

The packing efficiencies for the circular, elliptical and the novel hexagonal concentrators are calculated using the actual arrangements given in Figs. 3, 4 and 8 respectively, and equation (1). Figs. 6, 7 and 9 show the possible arrangements to improve their packing densities. All units are in cm.

Circular: [Fig. 3: $A_{ms} = 12.2 \times 12.2$, $A_{sc} = \pi r^2$, $r = 4/2 = 2$].
$eff_{Pd} = (N_{sc} \bullet A_{sc}) / A_{ms}$ x 100 % = $(9 \times \pi \times 4) / (12.2 \times 12.2) \times 100$ % = **76.0%**

Elliptical: [Fig. 4: $A_{ms} = 12.7 \times 18.6$, $A_{sc} = xy\pi$, $x = 3$, $y = 2$].
$eff_{Pd} = (N_{sc} \bullet A_{sc}) / A_{ms}$ x 100 % = $(9 \times 3 \times 2 \times \pi) / (12.7 \times 18.6) \times 100$ % = **71.8%**

3-D Hex: [Fig. 8: $A_{ms} = 18.1 \times 13$, $A_{sc} = (3/8)\,(3)^{1/2}\,(d_1)^2$, $d_1 = 6$].
$eff_{Pd} = (N_{sc} \bullet A_{sc}) / A_{ms} \times 100$ % = $(9 \times 3/8 \times (3)^{1/2} \times 36) / (18.1 \times 13) \times 100\%$ = **89.4%**

The results show that the novel 3-D Hex concentrator has a higher packing efficiency of 89.4% and therefore, has the potential of improving the performance of a static LCPV module. The square entrance geometry of Fig. 5 is calculated to give 95.7% packing efficiency which is 6.8% more than the hexagonal type. However, the interconnection between the hexagonal entrance apertures shows a better bonding, which is an important durability factor and makes it therefore superior to the square entry aperture geometry. Thus, the hexagonal concentrator is considered better in this study with the additional durability and aesthetic features.

B. Polar plot of 2-D Hex concentrator

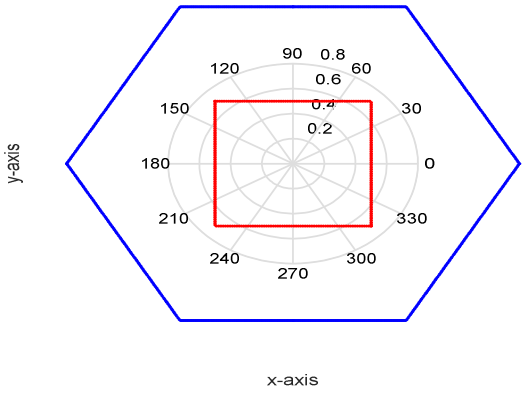

Fig. 12. 2-D Hex concentrator polar plot showing hexagonal entrance and square exit.

Fig. 12 shows the polar plot for the Hex concentrator with the square exit centrally positioned. The angular responses of both the hexagonal entry and square exit apertures are

displayed with θ, ranging from 0 to 360^0 with respect to the common radius r_c. Blending this with the height forms the 3-D Hex concentrator as demonstrated in Fig. 13.

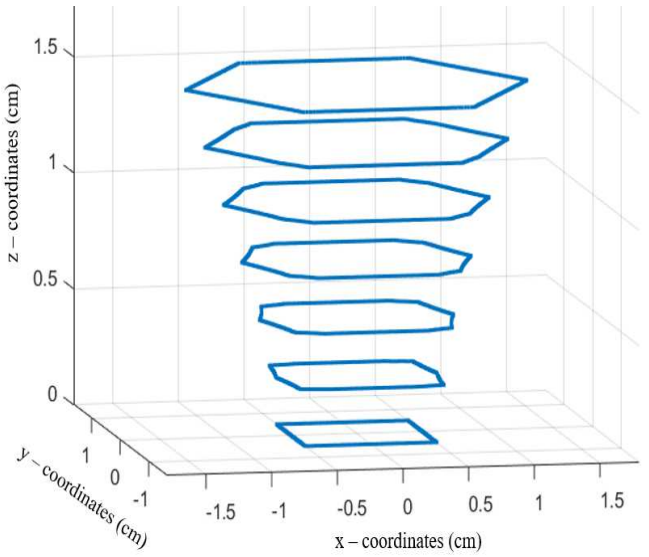

Fig. 13. 3-D Hex concentrator formation with low resolution of five concentric levels with concentrator height = 1.5 cm.

The formation from the square exit (bottom) to the desired hexagonal entrance aperture, with a very low resolution for seven formation stages is displayed here.

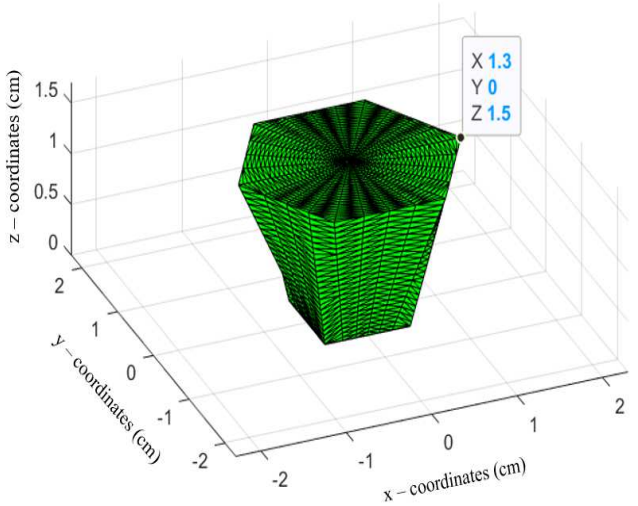

Fig. 14 3-D Hex concentrator formation with very high resolution of many concentric levels with concentrator height = 1.5 cm.

Fig. 14 shows a high-resolution plot of the novel 3-D Hex concentrator, using the *alphaShape function* in MATLAB. The hexagonal entrance entry and square exit geometries can be identified clearly. Given the height, the shape blends a square exit into a hexagonal entrance with multiple layers of the hexagonal shapes as the transformation begins with the square from the bottom into hexagon at the top (see Fig. 13). This is obtained according to the program which is based on the model design equations.

V. Conclusions

In this work, the importance of packing efficiency of solar concentrators in static nonimaging LCPV modules, for BICPV systems has been presented with the aim of improving the system performance. The proposed 3-D hexagonal entrance shape was compared with two alternative existing geometries and showed a relatively higher theoretical packing efficiency of 89.4% when compared with the elliptical (3-D SEH) and circular (3-D CPC) geometries, which have theoretical packing efficiencies of 71.8% and 76.0% respectively. This will have an impact on the overall electrical yield of an LCPV module as it offers a larger capture area for sunlight. Future works on the 3-D Hex concentrator shall include the optimisation of the side profile geometry, its optical characterisation and fabrication for experiments. Unfortunately, there is little or no existing work or literature on the subject considered in this paper, which makes this work the first of its kind.

References

[1] S. H. Abu-Bakar *et al.*, "Potential of implementing the low concentration photovoltaic systems in the United Kingdom," *Int. J. Electr. Comput. Eng.*, vol. 7, no. 3, pp. 1398–1405, 2017, doi: 10.11591/ijece.v7i3.pp1398-1405.

[2] N. Sellami and T. K. Mallick, "Optical characterisation and optimisation of a static Window Integrated Concentrating Photovoltaic system," *Sol. Energy*, vol. 91, pp. 273–282, 2013, doi: 10.1016/j.solener.2013.02.012.

[3] A. Alamoudi *et al.*, "Using static concentrator technology to achieve global energy goal," *Sustain.*, vol. 11, no. 11, pp. 1–22, Jun. 2019, doi: 10.3390/su11113056.

[4] D. Freier, R. Ramirez-iniguez, C. Gamio, T. Jafry, and F. Muhammad-sukki, "Optical Concentrators for Portable Solar Photovoltaic Systems for Developing Countries – A Review," *Renew. Sustain. Energy Rev.*, vol. 90, no. October 2016, pp. 957–968, 2018, doi: 10.1016/j.rser.2018.03.039.

[5] D. F. Raine, F. Muhammad-sukki, R. Ramirez-iniguez, J. A. Ardila-rey, T. Jafry, and C. Gamio, "Embodied Energy and Cost Assessments of a Concentrating Photovoltaic Module," pp. 1–15, 2021.

[6] H. Baig *et al.*, "Conceptual design and performance evaluation of a hybrid concentrating photovoltaic system in preparation for energy," *Energy*, vol. 147, no. December, pp. 547–560, 2018, doi: 10.1016/j.energy.2017.12.127.

[7] T. Cooper, F. Dähler, G. Ambrosetti, A. Pedretti, and A. Steinfeld, "Performance of compound parabolic concentrators with polygonal apertures," *Sol. Energy*, vol. 95, pp. 308–318, 2013, doi: 10.1016/j.solener.2013.06.023.

[8] D. Freier Raine, R. Ramirez-Iniguez, T. Jafry, F. Muhammad-Sukki, and C. Gamio, "Design method of a compact static nonimaging concentrator for portable photovoltaics using parameterisation and numerical optimisation," *Appl. Energy*, vol. 266, no. November 2019, p. 114821, 2020, doi: 10.1016/j.apenergy.2020.114821.